EFFICIENT NUMERICAL DYNAMIC ANALYSIS OF TENSION LEG PLATFORMS UNDER SEA WAVE LOADS

Mohammad Reza Tabeshpour [1] , Ali Akbar Golafshani [2] , Mohammad Saied Seif [3]

1- Ph.D. Candidate, Mech. Eng. Dept., Sharif University of Technology
2- Associate Professor, Mech. Eng. Dept., Sharif University of Technology
3- Associate Professor, Civil. Eng. Dept., Sharif University of Technology

Abstract

However it is possible to use of numerical methods such as beta-Newmark in order to investigate the structural response behavior of the dynamic systems under random sea wave loads but because of necessity to analysis the offshore systems for extensive time to fatigue study it is important to use of simple stable methods for numerical integration. The modified Euler method (MEM) is a simple numerical procedure which can be effectively used for the analysis of the dynamic response of structures in time domain. It is also very effective for response dependent systems in the field of offshore engineering. An important point is investigating the convergence and stability of the method for strongly nonlinear dynamic systems when high initial values for differential equation or large time steps are considered for numerical integrating especially when some frequencies of the system is very high. In this paper the stability of the method for solving differential equation of motion of a nonlinear offshore system (tension leg platform, TLP) under random wave excitation is presented. The key point of suitability of MEM for solving the TLP system is that the maximum frequency of the system is about 0.5 Hz. The stability criterion and the convergence of the numerical solution for critical time steps are numerically discussed.

Keywords: Tension leg platform - Ocean wave - Stochastic - Nonlinear

Introduction

It is obvious that there is a demand for oil exploitation in deep water. By increasing of water depth the environment will be more severe and therefore some innovative structures are required for economic production of gas and petroleum in deep water. An engineering idea is the minimization of the resistance of structure to environmental loads by making the structure flexible. This structural flexibility causes nonlinearity in structural stiffness matrix because of large deformations. Wave loading on the ocean structures is complex. Since they are compliant, these structures must be designed dynamically.

Fig. (1) shows different components of the TLP made up of vertical and horizontal elements on the upper structure and vertical tendons connecting the structure to a foundation on the seabed. The extra buoyancy over the platform weight ensures that the tendons are always kept in tension. As mentioned, the TLP is essentially a semi-submersible vessel which is moored to the sea floor by a number of pretensioned tendons. The tendons are connected at the sea floor to a template which is piled in place. It is significant to note that unlike the case of normal pile foundations, the piles experience tension rather than compression. The natural

periods of the structure in surge, away and yaw must be greater than the wave periods of significant energy. The heave, roll and pitch natural periods, on the other hand, being much shorter, must be less than the significant wave energy periods.

Angelides et al. (1982) considered the influence of hull geometry, force coefficients, water depth, pre-tension and tendon stiffness on the dynamic responses of the TLP. The floating part of the TLP was modeled as a rigid body with six degrees of freedom. The tendons were represented by linear axial springs. Wave forces were evaluated using a modified Morison equation on the displaced position of the structure considering the effect of the free sea surface variation.

Morgan and Malaeb (1983) investigated the dynamic response of TLPs using a deterministic analysis. The analysis was based on coupled nonlinear stiffness coefficients and closed-form inertia and drag-forcing functions using the Morison equation. The time histories of motions were presented for regular wave excitations. Chandrasekaran and Jain (2001 and 2002) investigate the structural response behavior of the triangular TLP under several random sea wave loads and current loads in both time and frequency domain. They study the effect of coupling of stiffness coefficients in the stiffness matrix and the effect of variable submergence of the structure, due to varying water surface, on the structural response of the triangular TLP.

A Comprehensive study on the results of tension leg platform responses in random sea considering all structural and excitation nonlinearities is presented [7]. This kind of interpretation of the results is necessary for optimum design of TLP.

There are several issues in design optimization of TLP. Geometrical optimum design of TLP hull is presented by using genetic algorithm method under regular sea waves [8]. Such a method can be used to extend the structural optimization under random wave loads. Optimum pretension of tendons can be determined based on minimum down time or maximum fatigue life. In minimum down time the nonlinear time histories of deformations and accelerations are investigated and in fatigue study it is used first order reliability method to estimate life time of tendons.

To work on the closed form solutions of TLP can be very useful to have a deep view of the structural behavior because of highly nonlinearities in the real structure. A continuous model for vertical motion of TLP considering the effect of continuous foundation has been reported [9]. The exact solution of the heave response of the structure can be useful both in initial design of tendons and verification of the complete coupled model responses.

Added mass fluctuation is a important point because of direct effect in life time of tendons when fatigue analyses are carried out. Fluctuating added mass has a direct relation to heave response of the hull structure. The effect of added mass fluctuation on the heave response of tension leg platform has been investigated by using perturbation method both for discrete and continues models [10-11]. Also the analytical solution derived can be used to verify the numerical results of the complete model.

Other important problem is investigation of the effects of radiation and scattering on the hull and tendon responses. An analytical solution for surge motion of TLP was proposed and demonstrated [12-14], in which the surge motion of a platform with pre-tensioned tethers was calculated. In that study, however, the elasticity of tethers was only implied and

the motion of tethers was also simplified as on-line rigid-body motion proportional to the top platform. Thus, both the material property and the mechanical behavior for the tether incorporated in the tension leg platform system were ignored. When this simplification was applied, no matter what the material used was or what the dimension of tethers was, the dynamic response of the platform would remain the same in terms of the vibration mode, periods and the vibration amplitude. An important point in that study was linearization of the surge motion. But it is obvious that the structural behavior in the surge motion is highly nonlinear because of large deformation of TLP in the surge motion degree of freedom (geometric nonlinearity) and nonlinear drag forces of Morison equation. Therefore the obtained solution is not true for the actual engineering application. For heave degree of freedom the structural behavior is linear, because there is not geometric nonlinearity in the heave motion degree of freedom and drag forces on legs have no vertical component. Similarly an analytical heave vibration of TLP with radiation and scattering effects for damped systems has been presented [15]. Similar method is presented for hydrodynamic pitch response of the structure [16].

An important computational problem in nonlinear dynamic analysis of structures under combined wave and wind excitation in order to fatigue analysis in wide domain of time is the efficiency on the numerical method used for time integration of equation of motion. It is discussed on the convergence and stability of the modified Euler method (MEM) for dynamic analysis of the structures that their frequencies are limited between two distinct upper and lower bounds [17].

A computer program (SNATELP) is developed to stochastic and nonlinear dynamic analysis capable of solving large displacement problem dynamically in the time domain based on Modified Euler method time integration.

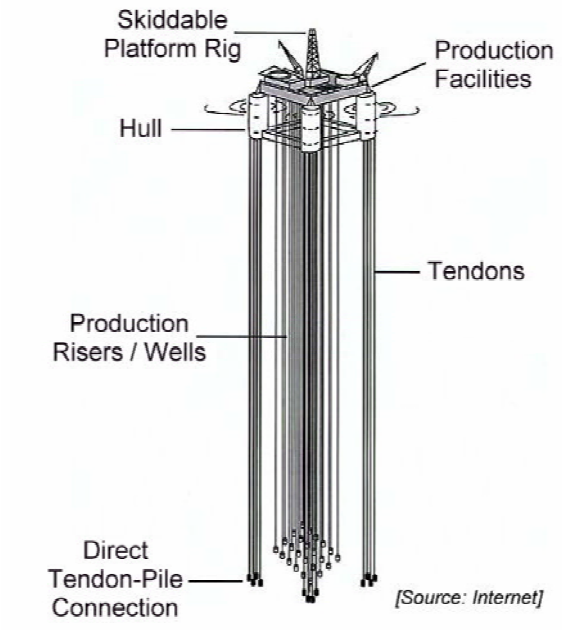

Fig. 1- TLP configuration and components

Equation of Motion

The equation of motion of the triangular TLP under a regular wave is given as:

$$[M]\{\ddot{X}\}+[C]\{\dot{X}\}+[K]\{X\}=\{F(t)\} \qquad (1)$$

where $[M],[C]$ and $[K]$ are the matrices of mass, damping and stiffness respectively, $\{X\}$, $\{\dot{X}\}$ and $\{\ddot{X}\}$ are the structural displacement, velocity and acceleration vector respectively and $F(t)\}$ is the excitation force vector.

Mass matrix, [M]

Structural mass is assumed to be lumped at each degree of freedom. Hence, it is diagonal in nature and is constant. The added mass, M_a, due to the

water surrounding the structural members and arising from the modified Morrison equation is considered up to the mean sea level (MSL) only. The fluctuating component of added mass due to the variable submergence of the structure in water is considered in the force vector depending upon whether the sea surface elevation is above (or) below the MSL. The mass matrix of TLP is

$$[M]=\begin{array}{c}\begin{vmatrix} Surge & Sway & Heave & Roll & Pitch & Yaw \end{vmatrix}\\ \begin{bmatrix} M'_{SS} & 0 & 0 & 0 & 0 & 0 \\ 0 & M'_{WW} & 0 & 0 & 0 & 0 \\ 0 & 0 & M'_{HH} & 0 & 0 & 0 \\ M_{aRS} & M_{aRW} & M_{aRH} & M_{RR} & 0 & 0 \\ M_{aPS} & M_{aPW} & M_{aPH} & 0 & M_{PP} & 0 \\ 0 & 0 & 0 & 0 & 0 & M_{YY} \end{bmatrix}\end{array} \quad (2)$$

where $M_{SS}=M_{WW}=M_{HH}=M$ and $M'_{SS}=M_{SS}+M_{aSS}$ and $M'_{WW}=M_{WW}+M_{aWW}$ and $M'_{HH}=M_{HH}+M_{aHH}$. M is the total mass of the entire structure, M_{RR} is the total mass moment of inertia about the x axis = Mr_x^2, M_{PP} is the total mass moment of inertia about the y axis = Mr_y^2, M_{YY} is the total mass moment of inertia about the z axis = Mr_z^2, r_x is the radius of gyration about the *x* axis, r_y is the radius of gyration about the *y* axis, and r_z is the radius of gyration about the *z* axis. The added mass terms are:

$$\begin{aligned} dM_{aSS} &= dM_{aWW} = dM_{aHH} \\ &= 0.25\pi D^2 (C_m - 1)\rho\, dl \end{aligned} \quad (3)$$

$$M_{aSS} = \int_{lenght} dM_{aSS} \quad (4)$$

M_{aRS} is the added mass moment of inertia in the roll degree of freedom due to hydrodynamic force in the surge direction. M_{aRW} is the added mass moment of inertia in the roll degree of freedom due to hydrodynamic force in the sway direction. M_{aRH} is the added mass in the roll degree of freedom due to hydrodynamic force in the heave direction. M_{aPS} is the added mass moment of inertia in the pitch degree of freedom due to hydrodynamic force in the surge direction. M_{aPW} is the added mass moment of inertia in the pitch degree of freedom due to hydrodynamic force in the sway direction. M_{aPH} is the added mass in the pitch degree of freedom due to hydrodynamic force in the heave direction. The presence of off diagonal terms in the mass matrix indicates a contribution in the added mass due to the hydrodynamic loading. The loading will be attracted only in the surge, heave and pitch degrees of freedom due to the unidirectional wave acting in the surge direction on a symmetric configuration of the platform about the *x* and *z* axes).

Stiffness matrix of the TLP

The coefficients, K_{AB}, of the stiffness matrix of the triangular TLP are derived as the reaction in the degree of freedom *A* due to unit displacement in the degree of freedom *B*, keeping all other degrees of freedom restrained. The coefficients of the stiffness matrix have nonlinear terms due to the cosine, sine, square root and squared terms of the displacements. Furthermore, the tendon tension changes due to the motion of the TLP in different degrees of freedom makes the stiffness matrix response-dependent. The stiffness matrix [*K*] of a TLP is:

$$[K]=\begin{array}{c}\begin{vmatrix} Surge & Sway & Heave & Roll & Pitch & Yaw \end{vmatrix}\\ \begin{bmatrix} K_{SS} & 0 & 0 & 0 & 0 & 0 \\ 0 & K_{WW} & 0 & 0 & 0 & 0 \\ K_{HS} & K_{HW} & K_{HH} & K_{HR} & K_{HP} & K_{HY} \\ 0 & K_{RW} & 0 & K_{RR} & 0 & 0 \\ K_{PS} & 0 & 0 & 0 & K_{PP} & 0 \\ 0 & 0 & 0 & 0 & 0 & K_{YY} \end{bmatrix}\end{array} \quad (5)$$

In the stiffness matrix the presence of off-diagonal terms, reflects the coupling effect between the various degrees of freedom and the coefficients depend on the change in the tension of the tendons, which is affecting the buoyancy of the system. Hence, the [*K*] is not constant for all time instants but the coefficients are replaced by a new value computed at each time instant depending upon the response value at that time instant. The stiffness matrix of the four-legged square TLP is taken as suggested by Morgan and Malaeb (1983).

Stiffness of Surge direction (Fig. 2)

By giving an arbitrary displacement *x* in the surge direction, the increase in the initial pre-tension, in each leg, is given by:

$$\Delta T_{surge} = \left(\sqrt{x^2 + l^2} - l\right) AE / l \qquad (6)$$

where *A* is the cross-sectional area of the tether, *E* is Young's Modulus of the tether, ΔT_{surge} is the increase in the initial pre-tension due to the arbitrary displacement given in the surge degree of freedom, *l* is the length of the tether, and *x* is the arbitrary displacement in the surge degree of freedom.
Equilibrium of forces in the surge direction gives.

$$K_{SS}\, x = n(T_0 + \Delta T_{surge}) \sin\phi_x \qquad (7)$$

where T_0 is the initial pre-tension in the tether, and ϕ_x is the angle between the initial and the displaced position of the tether for unit displacement given in the surge direction.

$$\sin\phi_x = \frac{x}{\sqrt{x^2 + l^2}} \qquad (8)$$

Putting Eq. (8) in Eq. (7), we get:

$$K_{SS} = \frac{n(T_0 + \Delta T_{surge})}{\sqrt{x^2 + l^2}} \qquad (9)$$

Equilibrium of forces in the heave direction gives:

$$K_{HS} = nT_0(\cos\phi_x - 1) + n\Delta T_{surge} \cos\phi_x \qquad (10)$$

where

$$\cos\phi_x = \frac{l}{\sqrt{x^2 + l^2}} \qquad (11)$$

Rearranging terms, we get:

$$K_{HS} = \frac{\left(nT_0(\cos\phi_x - 1) + n\Delta T_{surge} \cos\phi_x\right)}{x} \qquad (12)$$

or

$$K_{HS} = \frac{\left(nT_0(l - \sqrt{x^2 + l^2}) + n\Delta T_{surge}\, l\right)}{x\sqrt{x^2 + l^2}} \qquad (13)$$

Summation of moments along the pitch direction gives:

$$K_{PS}\, x = -K_{SS}\, x\bar{h} \text{ or } K_{PS} = -K_{SS}\bar{h} \qquad (14)$$

where $\bar{h}$ is the distance of the center of gravity (CG) from the base of the pontoon. The force $K_{SS}\, x$ acts at the bottom of hull and gives rise to a moment along pitch direction which is considered at CG. The negative sign occurs due to counterclockwise moment $K_{SS}\, x\bar{h}$.

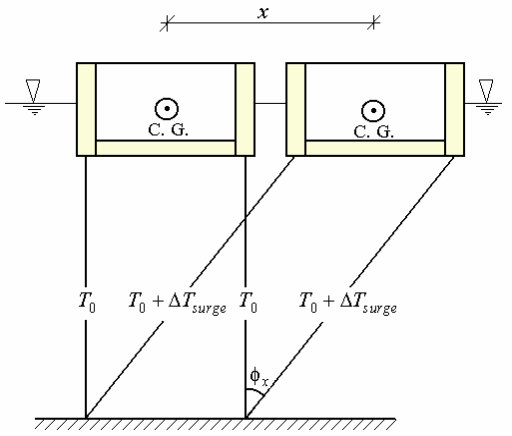

Fig. 2- Displacement in surge degree of freedom

Stiffness of Heave direction

By giving an arbitrary displacement *z* in the heave direction, the equilibrium of forces in the heave direction gives:

$$K_{HH} z = n\left(\frac{AE}{l} + \frac{\rho\pi g D_c^2}{4}\right) z \qquad (15)$$

or

$$K_{HH} = n\left(\frac{AE}{l} + \frac{\rho\pi g D_c^2}{4}\right) \qquad (16)$$

where g is the acceleration due to gravity, ρ is the mass density of water and D_c is the diameter of the column.

Stiffness of Roll direction (Fig. 3)

By giving an arbitrary rotation θ_x in the roll degree of freedom and assuming symmetry, the change in the initial pretension, in each leg, is given by:

$$\Delta T_{roll} = \frac{AE}{l} b \cos\theta_x(\theta_x) = -\Delta T'_{roll} \qquad (17)$$

Summation of the moments of the resulting forces about the *x*-axis gives:

$$K_{RR} = n\left(\rho\pi g b^2 \frac{D_c^2}{4} + T_0 \bar{h} \frac{\sin\theta_x}{\theta_x} + AEb^2 \frac{\cos\theta_x}{L}\right) \qquad (18)$$

Equilibrium of forces in the heave direction gives:

$$K_{HR} = \frac{2(\Delta T_{roll} + \Delta T'_{roll})}{\theta_x} = 0 \qquad (19)$$

where ΔT_{roll} is the increase in the initial pre-tension in the tether due to the arbitrary rotation given in the roll degree of freedom, $\Delta T'_{roll}$ is the increase in the initial pre-tension in the farther tether due to the arbitrary rotation given in the roll degree of freedom.

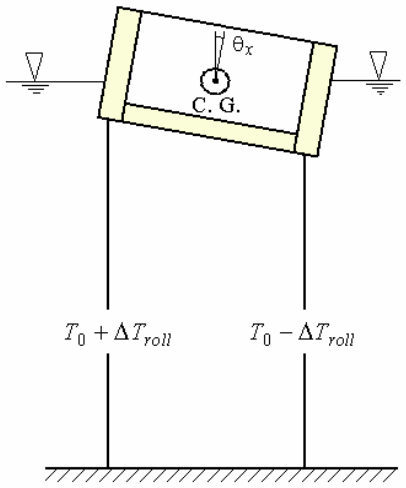

Fig. 3- Displacement in roll degree of freedom

Damping matrix, [C]

Assuming [*C*] to be proportional to [*K*] and [*M*], the elements of [*C*] are determined by the equation given below, using the orthogonal properties of [*M*] and [*K*]:

$$C = \alpha M + \beta K \qquad (20)$$

α and β are constant. This matrix is calculated based on the initial values of [*K*] and [*M*] only.

Hydrodynamic force vector, {F(t)}

The problem of suitable representation of the wave environment or more precisely the wave loading is the problem of prime concern. Once the wave environment is evaluated, wave loading on the structure may be computed based on suitable theory. In this work the water particle position η is determined according to Airy's linear wave theory:

$$\eta(x,t) = A\cos(kx - \omega t) \qquad (21)$$

where *A* is the amplitude of the wave, *k* is the wave number, ω is the wave frequency and *x* is the horizontal distance from the origin.

In order to incorporate the effect of variable submergence which is an

important aspect of hydrodynamic loading on TLP, Chakarbarti's approach will be adopted in which instantaneous sea surface elevation is taken as the still water level (or water depth). The fluctuating free surface effect can be significant when the wave height cannot be ignored in comparison to the water depth. Chakarbarti (1971) suggested the following form of the water particle velocity $\dot{u}$

$$\dot{u} = A\omega\cos(kx-\omega t)\frac{\cosh(kz)}{\sinh(d+\eta)} \qquad (22)$$

where η is the instantaneous water surface elevation and is given as Eq. (1). likewise, the water particle acceleration also gets modified.

In stochastic modeling, sea waves are commonly characterized by their PSDFs. Water particle kinematics, at different location on the structure, are considered to be derived processes and these need not be specified in addition to the sea surface elevation. By considering the random process as a linear superposition of a large number of independent waves, its distribution becomes Gaussian. Depending upon the fetch conditions, several analytical expressions exist for the approximation of the sea surface elevation spectrum (i.e. its PSDF). A well-known spectrum model for ocean waves is Peirson-Moskowitz (P-M) model. The modified P-M spectrum model is assumed to adequately represent the sea state. It is given by:

$$S_{\eta\eta}(\omega) = \frac{H_s^2 T_z}{8\pi^2}\left\{\frac{T_z\omega}{2\pi}\right\}^{-5}\exp\left\{-\frac{1}{\pi}\left(\frac{T_z\omega}{2\pi}\right)^{-4}\right\} \qquad (23)$$

where H_s is the significant wave height in m, T_z is zero up crossing period in s and ω is the angular frequency.

The linearized small-amplitude wave theory allows the summation of velocity potential, wave elevation, and water particle kinematics of the individual regular wave to form a random wave made up of a number of components. The generated synthetic random wave is considered to be adequately represented by a summation of linear harmonic regular waves. The series representation of sea surface elevation is given by the equation

$$\eta(x,t) = \lim\sum_{i=1}^{k} A_i\cos(k_i x-\omega_i t+\phi_i) \qquad (24)$$

$$A_i = \sqrt{2S_{\eta\eta}(\omega_i)\Delta\omega_i} \qquad (25)$$

where A_i is the amplitude of the *i*-th component wave, k_i is the wave number of the *i*-th component wave, ω_i is the wave frequency of the *i*-th component wave, ϕ is the phase angle of the *i*-th component wave, varying between 0 and 2π, x is the horizontal distance from the origin and $S_{\eta\eta}(\omega)$ is the one-sided sea surface elevation PSDF. Based on these studies, the asymptotic approach to the Gaussian distribution is found to be slow for a number of component waves over about 75. The time interval Δt is set to satisfy the condition $\Delta t \le 2\pi/5\omega_{\max}$. Keeping in view the natural period of the structure, the value of Δt is chosen as 0.5 s, which is much smaller than required. The length of the simulated wave record is controlled so that about 4096 data points are generated in one run. For the random wave, when the response is to be found by simulation, the total period of simulated loading of 2048 s is chosen which gives 4096 (2^{12}) data points.

Once the sea surface elevation time history $\eta(x,t)$ is known from Eq. (24), the time histories of the water particle velocity and acceleration are computed by wave superposition, according to Airy's linear wave theory. The horizontal water particle velocity $\dot{u}(\xi,z,t)$ and the vertical water particle velocity $\dot{w}(\xi,z,t)$ are given as:

$$\dot{u}(\xi,z,t) = \sum_{i=1}^{k} A_i\omega_i \cos(k_i\xi - \omega_i t + \phi_i)\frac{\cosh(k_i z)}{\sinh(k_i(d+\eta_i))} \quad (26)$$

$$\dot{w}(\xi,z,t) = \sum_{i=1}^{k} A_i\omega_i \sin(k_i\xi - \omega_i t + \phi_i)\frac{\sinh(k_i z)}{\sinh(k_i(d+\eta_i))} \quad (27)$$

And related accelerations are:

$$\ddot{u}(\xi,z,t) = \sum_{i=1}^{k} A_i\omega_i^2 \cos(k_i\xi - \omega_i t + \phi_i)\frac{\cosh(k_i z)}{\sinh(k_i(d+\eta_i))} \quad (28)$$

$$\ddot{w}(\xi,z,t) = \sum_{i=1}^{k} A_i\omega_i^2 \sin(k_i\xi - \omega_i t + \phi_i)\frac{\sinh(k_i z)}{\sinh(k_i(d+\eta_i))} \quad (29)$$

where:

$$x = \xi\cos\alpha_x \quad (30\text{-}1)$$

$$y = \xi\sin\alpha_x \quad (30\text{-}2)$$

where k_i is the i-th component wave number, y is the vertical distance at which the wave kinematics is calculated, d is the water depth, η is the sea surface elevation, which is equal to $\eta(x,t)$ given by Eq. (24). where α_z is angle of the axis to vertical and α_x is angle of the cylinder projection to the x-axis. The wave forces acting on the cylindrical member of the TLP structure are obtained by using modified Morison's equation, which takes relative velocity and acceleration between the structure and water particles into account.

For cylindrical structural components, oriented in an arbitrary direction, the velocity vector $\{\dot{U}_N\}^T = \{\dot{u}_x, \dot{u}_y, \dot{u}_z\}$ and acceleration vector $\{\ddot{U}_N\}^T = \{\ddot{u}_x, \ddot{u}_y, \ddot{u}_z\}$, acting perpendicular to the cylindrical axis, arise from the vectors of the orbital velocities $\{\dot{U}\}^T = \{\dot{u}, 0, \dot{w}\}$ and accelerations $\{\ddot{U}\}^T = \{\ddot{u}, 0, \ddot{w}\}$, and from the unit tangent vector in the direction of the cylinder axis

$$\{C\}^T = \{C_x, C_y, C_z\} = \{\sin\alpha_z\cos\alpha_x, \sin\alpha_z\sin\alpha_x, \cos\alpha_z\} \quad (31)$$

From this, one deduces the velocity and acceleration components

$$\dot{u}_x = \dot{u} - C_x(C_x\dot{u} + C_z\dot{w}) \quad (32\text{-}1)$$

$$\ddot{u}_x = \ddot{u} - C_x(C_x\ddot{u} + C_z\ddot{w}) \quad (32\text{-}2)$$

$$\dot{u}_y = -C_y(C_x\dot{u} + C_z\dot{w}) \quad (32\text{-}3)$$

$$\ddot{u}_y = -C_y(C_x\ddot{u} + C_z\ddot{w}) \quad (32\text{-}4)$$

$$\dot{u}_z = \dot{w} - C_z(C_x\dot{u} + C_z\dot{w}) \quad (32\text{-}5)$$

$$\ddot{u}_z = \ddot{w} - C_z(C_x\ddot{u} + C_z\ddot{w}) \quad (32\text{-}6)$$

and the velocity magnitude

$$\left|\{\dot{U}_N\}\right| = \sqrt{\dot{u}_x^2 + \dot{u}_y^2 + \dot{u}_z^2} \quad (33)$$

or

$$\left|\{\dot{U}_N\}\right| = \sqrt{\dot{u}^2 + \dot{w}^2 - (C_x\dot{u} + C_z\dot{w})^2} \quad (34)$$

The components of the wave force per unit length are as follows

$$f_x = C_m\rho_w\frac{\pi D^2}{4}\ddot{u}_x + C_d\frac{\rho_w}{2}D\left|\{\dot{U}_N^e\}\right| \times (\dot{u}_x - \dot{x} + \dot{u}_{cx}) \pm \frac{\pi D^2}{4}(C_m - 1)\rho_w\ddot{x} \quad (35\text{-}1)$$

$$f_y = C_m\rho_w\frac{\pi D^2}{4}\ddot{u}_y + C_d\frac{\rho_w}{2}D\left|\{\dot{U}_N^e\}\right| \times (\dot{u}_y - \dot{y} + \dot{u}_{cy}) \pm \frac{\pi D^2}{4}(C_m - 1)\rho_w\ddot{y} \quad (35\text{-}2)$$

$$f_z = C_m\rho_w\frac{\pi D^2}{4}\ddot{u}_z + C_d\frac{\rho_w}{2}D\left|\{\dot{U}_N^e\}\right| \times (\dot{u}_z - \dot{z}) \pm \frac{\pi D^2}{4}(C_m - 1)\rho_w\ddot{z} \quad (35\text{-}3)$$

$\dot{u}_c$ is the current velocity and β is the angle of current direction with x-axis

$$\dot{u}_{cx} = \dot{u}_c\cos\beta \quad (36\text{-}1)$$

$$\dot{u}_{cy} = \dot{u}_c\sin\beta \quad (36\text{-}2)$$

$$\left|\{\dot{U}_N^e\}\right| = \sqrt{(\dot{u}_x - \dot{x} + \dot{u}_{cx})^2 + (\dot{u}_y - \dot{y} + \dot{u}_{cy})^2 + (\dot{u}_z - \dot{z})^2} \quad (37)$$

x, *y* and *z* are displacements of the structure along with the *x*, *y*, and *z* axes respectively. The force vector {F(t)} is given as:

$$\{F(t)\} = \{F_x, F_y, F_z, M_x, M_y, M_z\}^T \quad (38)$$

The hydrodynamic force attracted by the members in the surge, sway and heave degrees of freedom are computed and designated as F_x, F_y and F_z, respectively.

$$\text{Surge Force} = \mathrm{F_x} = \left[\sum_{k=1}^{n}\{F_D(K) + F_I(K)\}\right]_{Column} \times \cos\alpha + [F_{d_x} + F_{i_x}]_{hull} \quad (39)$$

$$\textit{Sway}\ \text{Force} = \mathrm{F_y} = \left[\sum_{k=1}^{n}\{F_D(K) + F_I(K)\}\right]_{Column} \times \sin\alpha + [F_{d_y} + F_{i_y}]_{hull} \quad (40)$$

$$\textit{Heave}\ \text{Force} = \mathrm{F_z} = [F_v]_{Column} + [F_{d_z} + F_{i_z}]_{hull} \quad (41)$$

where F_x, F_y and F_z are the total forces in the *x*, *y* and *z* directions. $\sum_{k=1}^{n}$ is the summation over the vertical column of the drag force $F_D(K)$ and inertia force $F_I(K)$. *K* is the number segments of the of columns. The moment of these forces about the *x*, *y* and *z* axes are designated as M_x, M_y and M_z, respectively. The wave induced loading in the *x*, *y* and *z* directions on the vertical columns and hull causes surge, sway and heave components. Drag and inertia loading on the hull and vertical column members also cause moments about the *x*, *y* and *z*-axes, they are termed roll, pitch and yaw moments, respectively. The angle of wave incidence is denoted by α. F_{d_x} and F_{i_x} are the total drag and inertia forces in the *x* direction acting on the hull. Similarly, in the *y* direction, all the forces due to drag and inertia on the hull and columns induce total sway force F_y. F_{d_z} and F_{i_z} are the total drag and inertia forces on the hull in the vertical direction. F_v is the total vertical dynamic pressure forces on the column bottom. These horizontal and vertical drag and inertia forces cause moments about *x*, *y* and *z* axes, as under pitch moment

$$\mathrm{M_x} = \left[\sum_{k=1}^{n}\{M_D(k) + M_I(k)\}\right]_{Column} \sin\alpha + [M_{v_x} + M_{h_x}]_{hull} + [M_{p_x}]_{Column} \quad (42)$$

roll moment,

$$\mathrm{M_y} = \left[\sum_{k=1}^{n}\{M_D(k) + M_I(k)\}\right]_{Column} \cos\alpha + [M_{v_y} + M_{h_y}]_{hull} + [M_{p_y}]_{Column} \quad (43)$$

yaw moment,

$$M_z = \sum_{k=1}^{n}[F_D(k) + F_I(k)]\, y_k \quad (44)$$

M_D and M_I are the moments due to horizontal forces on the TLP columns about axes perpendicular to the wave direction. M_{h_x}, M_{v_x}, and M_{h_y}, M_{v_y} are the moments due to horizontal and vertical hull forces about the *x* and *y* axes, respectively. M_{p_x} and M_{p_y} are the moments of the dynamic pressure, on the column bases, about the x and y axes. y_k is the moment arm from the k^{th} column for moments about the *z*-axis.

The modified Euler method (MEM)

Euler method is rarely used but knowing it is a staring point toward further examination of the methods of this class. The graphic presentation is shown in figure 4.

There is a known point of coordinates (x_m, y_m) lying on the wanted curve. A curve with a slope is drawn through this point

$$y'_m = f(x_m, y_m) \quad (45)$$

We can assume that y_{m+1} equals to the ordinate at the crossing point of L_1 and the straight line $x = x_{m+1} = x_m + h$. The equation of the straight line L_1 is:

$$y = y_m + y'_m(x - x_m) \tag{46}$$

and since

$$x_{m+1} - x_m = h \tag{47}$$

then

$$y_{m+1} = y_m + hf(x_m - y_m) \tag{48}$$

The error in $x = x_{m+1}$ is designated on the figure by *e*.

The last formula assigns the Euler method. Its characteristic is the big error from disruption and instability in some cases, i.e. a small error from rounding increases with the increase of *x*.

The modified Euler method is based on finding the average value of the slopes of the tangent lines in the points (x_m, y_m) and $(x_m + h, y_m + hy'_m)$. Graphically the method is presented on Fig. 5.

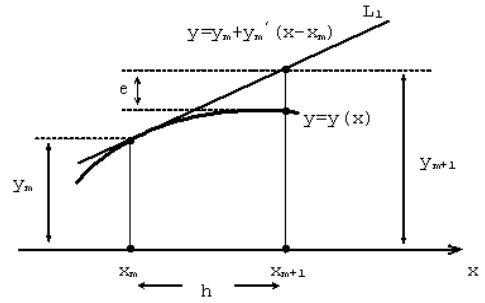

Fig. 4- Geometric presentation of Euler method

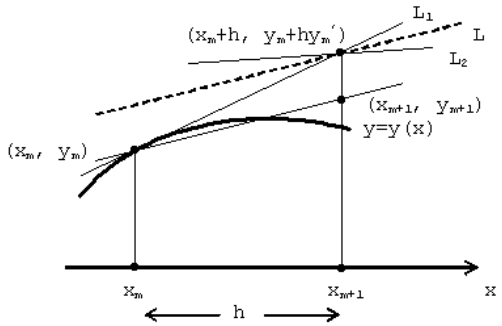

Fig. 5- Geometric presentation of the MEM

The slope of the straight line *L* is:

$$\Phi(x_m, y_m, h) = \frac{1}{2}\left[f(x_m, y_m) + f(x_m + h, y_m + hy'_m)\right] \tag{49}$$

where: $y'_m = f(x_m, y_m)$

The equation for *L* is assigned as:

$$y = y_m + (x - x_m)\Phi(x_m, y_m, h) \tag{50}$$

$$y_{m+1} = y_m + h\Phi(x_m, y_m, h) \tag{51}$$

The last equations express the MEM.

Application of MEM in structural dynamics

Consider the numerical evaluation of the free-vibrational response of a linear, undamped, simple mass-spring system governed by the following differential equation:

$$\ddot{x} + \omega^2 x = 0 \tag{52}$$

in which *x* is the displacement of the system; ω is the circular natural frequency of vibration of the system; and a dot superscript denotes differentiation with respect to time, *t*. Let x_n and $\dot{x}_n$ be the known displacement and velocity, respectively, of the system at time t_n. This time is expressed in terms of a non-negative integer number, *n*, and a time step, Δt, as $t_n = n\Delta t$. By application of the MEM, the displacement and velocity of the system, x_{n+1} and $\dot{x}_{n+1}$, at time $t_{n+1} = (n+1)\Delta t$, are evaluated as follows. By using equation (52), compute

$$\ddot{x}_n = -\omega^2 x_n \tag{53}$$

Then, compute

$$\dot{x}_{n+1} = \dot{x}_n + \ddot{x}_n \Delta t \tag{54}$$

Now there is two approaches in order to calculate $\dot{x}_{n+1}$. First approach is using only the velocity in time step *n*+1:

$$x_{n+1} = x_n + \dot{x}_{n+1}\,\Delta t \tag{55}$$

The second one is averaging of velocities of two steps:

$$x_{n+1} = x_n + \frac{\dot{x}_{n+1} + \dot{x}_n}{2}\Delta t \tag{56}$$

If one uses the following equation

$$x_{n+1} = x_n + \dot{x}_n\,\Delta t \tag{57}$$

then the method is called Euler method. With the values of x_{n+1} and $\dot{x}_{n+1}$ available, the procedure defined by equations (53)-(55 or 56) may be repeated to compute the response of the system for subsequent discrete times larger than t_{n+1}. These computations can be carried out accurately by a proper implementation of the MEM. It is important to note that, in the MEM, the solution for x_{n+1} is based on using the equilibrium equation at time t_n. Therefore, the MEM is an explicit method. It is also important to note in equation (55) that the displacement x_{n+1} is computed by using the velocity $\dot{x}_{n+1}$. If $\dot{x}_{n+1}$ is replaced in equation (55) with $\dot{x}_n$, then the procedure defined by equations (53)-(55) reduces to the well known standard Euler method, which is an unstable approach that should never be used for structural dynamics applications [2].

Stability analysis for the MEM

the following characteristic equation is obtained:

$$\lambda^2 - (2 - \Delta t^2\,\omega^2)\lambda + 1 = 0 \tag{58}$$

and the roots of equation (58), λ_1 and λ_2 are

$$\lambda_1 = (1 - 0.5\Delta t^2\,\omega^2) + 0.5\Delta t\,\omega(\Delta t^2\,\omega^2 - 4)^{1/2} \tag{59}$$

$$\lambda_2 = (1 - 0.5\Delta t^2\,\omega^2) - 0.5\Delta t\,\omega(\Delta t^2\,\omega^2 - 4)^{1/2} \tag{60}$$

There are three important cases: in Case l, the roots are real-valued and distinct; in Case 2, the roots are real-valued and equal; and in Case 3, the roots are complex-valued quantities. Cases 1 and 2 lead to unstable solutions for x_n; and Case 3, which leads to stable solutions, is obtained if

$$\Delta t^2\omega^2 < 4 \tag{61}$$

This expression gives the condition for the stability of the MEM and may be reformulated as

$$\Delta t < \frac{T}{\pi} \tag{62}$$

in which $T = 2\pi/\omega$ is the natural period of vibration of the system. Therefore, the MEM is stable only when equation (62) is satisfied.
Similar calculation and considering eq. (56) instead of (55) results in

$$\Delta t < \frac{2T}{\pi} \tag{63}$$

Because of large displacement of TLP and nonlinear terms in exciting force, the equation of motion of TLP is strongly nonlinear and the exciting wave force is response dependent as well. Convergence and stability of the MEM has been investigated both analytically and numerically [17]. As a brief review it is presented the results of a case study investigated by Tabeshpour et al. Eigenvalue analysis results the following periods: Surge: 72.8 sec; Sway: 72.8 sec ; Heave: 2.44 sec; Roll: 2.16 sec; Pitch: 2.16 sec; and Yaw: 87.8 sec [17]. Deformations and accelerations of all degrees of freedom are illustrated in Figs. 6 and 7for 500 seconds. However the initial values are really high but after about 200 seconds the structural responses reach to a steady state. The more the period the fewer cycles required to reach to the steady state.

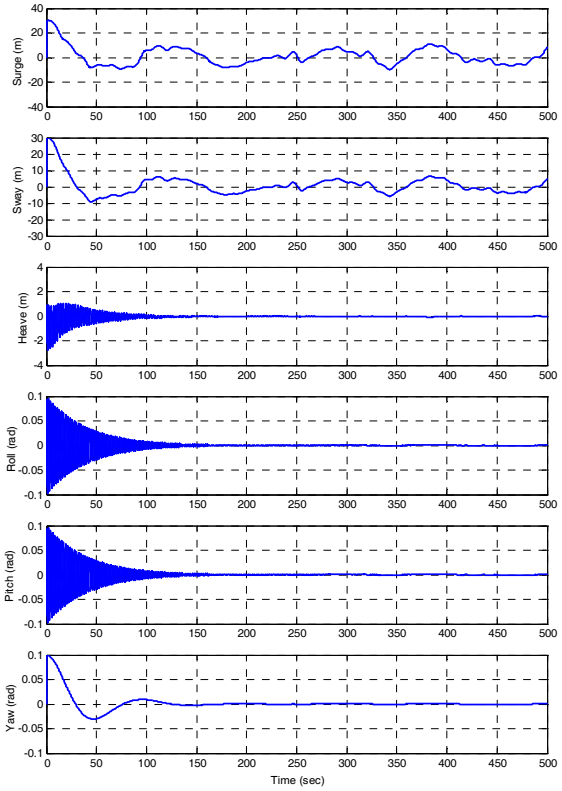

Fig. 6- Time history of displacements

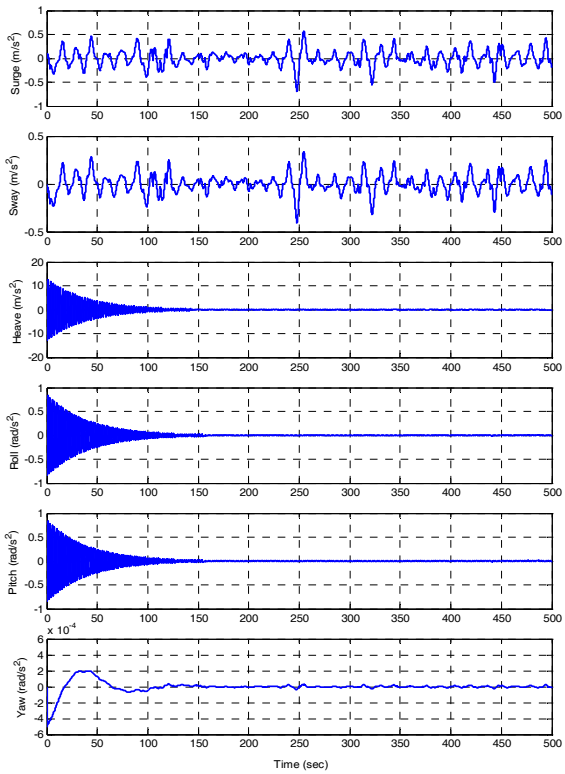

Fig. 7- Time history of accelerations

Numerical Study

A TLP in 400 *m* deep water has been chosen for the numerical study. The characteristics of the TLP under study are:

Diameter of Columns(m), $D_c = 18m$;

Diameter of Pontoon(m), $D = 12m$;

Pre-tension, $T_0 = 0.55E5\,KN$;

Length=90 *m*;

Tether tensions are assumed to be equally distributed in all the four tethers. TLP structure is assumed to behave like a rigid body. The stiffness matrix developed takes into account large deformations and other nonlinearities like tether tension, etc. And:

$H_s = 10\ m$, $T_z = 15$ sec

The angle of incident wave with x direction is 30°.

Eigenvalue analysis results the following periods:

Surge: 78.7 sec (0.08 rad/sec);

Sway: 78.7 sec (0.08 rad/sec);

Heave: 2.0 sec (3.14 rad/sec);

Roll: 1.8 sec (3.49 rad/sec);

Pitch: 1.8 sec (3.49 rad/sec); and

Yaw: 74.2 sec (0.085 rad/sec).

Based on the mentioned formulation, random surface elevation has been derived.

Then nonlinear dynamic analysis has been carried out and useful results have been achieved. Displacement of various degrees of freedom is illustrated in Fig. (8). It is seen low and high frequency component of motions illustrating the wave and structural period. In surge motion there is approximately 7 cycles in 500 seconds. It means that every global cycle has been occurred in time equal to surge period (78.7 sec). Similar result is seen for sway, roll, pitch and yaw motions.

A smooth motion occurred in 15 sec (T_z) is seen in surge, sway, heave and yaw motions. Because of coupling between heave and surge, heave motion is

affected by the frequency of surge degree of freedom. But in roll and pitch the period of high frequency component is equal to 1.8 sec (roll and pitch period). Also it is seen that yaw rotation is more than that of pitch and roll, because of no restriction in yaw degree of freedom.

An important parameter for desired serviceability, is acceleration. This parameter is shown in Fig. (9). The importance of acceleration goes back to the human and equipment sensitivity to vertical acceleration. Heave, roll and pitch accelerations are important to study and investigate the serviceability and performance of the system. A phenomenon similar to beating is clear in roll and pitch accelerations. The period of beating is equal to the structural period of surge and sway (78.7 sec). Such phenomenon is not seen in yaw motion because the period of yaw very long (74.2 sec).

A smooth motion occurred in 15 sec (T_z) is seen in surge, sway and yaw motions. The period of high frequency component in heave degree of freedom is equal to 2 sec (heave period) and similarly for roll and pitch motion the period of acceleration is equal to 1.8 sec (roll and pitch period)

In order to get a deep view on energy of motion one can use power spectral density (PSD) diagrams of various degrees of freedom (Fig. 10). The significant amplitude of surge and sway motion occur in the neighbor of 0.8 rad/sec (related to surge and sway period equal to 78.7 sec). Similar results are seen for other degrees of freedom because of coupling with surge and sway. There is a clear peak in frequency equal to 0.42 rad/sec related to T_z.

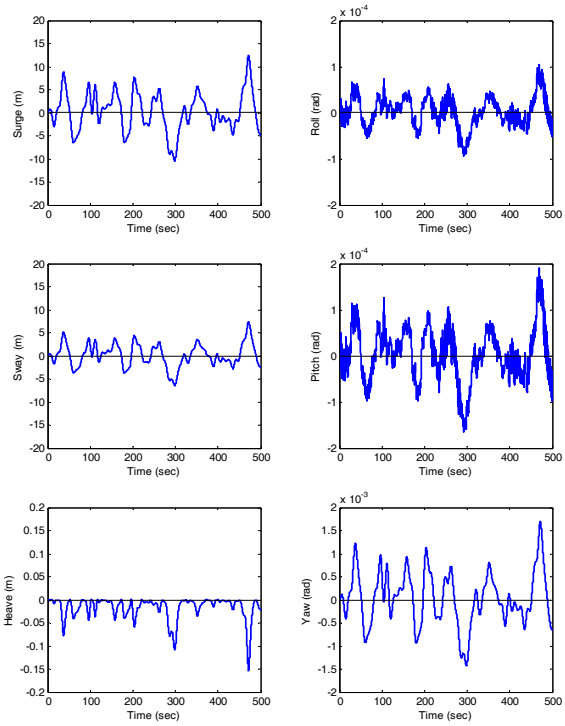

Fig. 8- Time history of Displacements

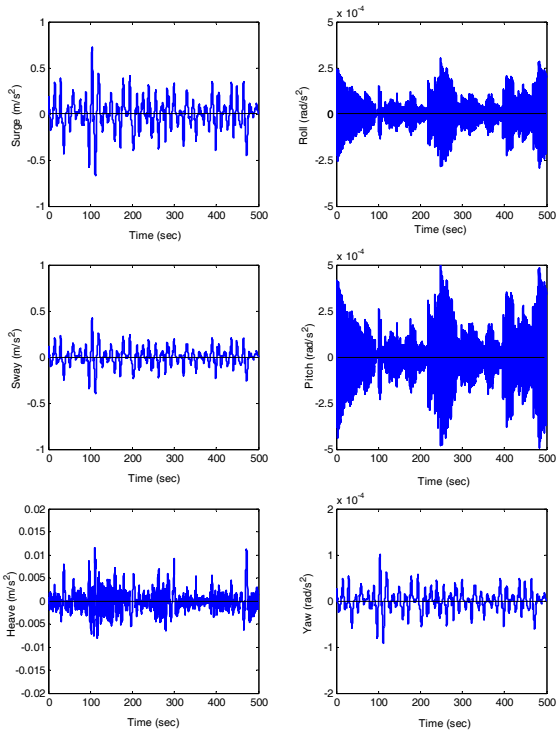

Fig. 9- Time history of acceleration

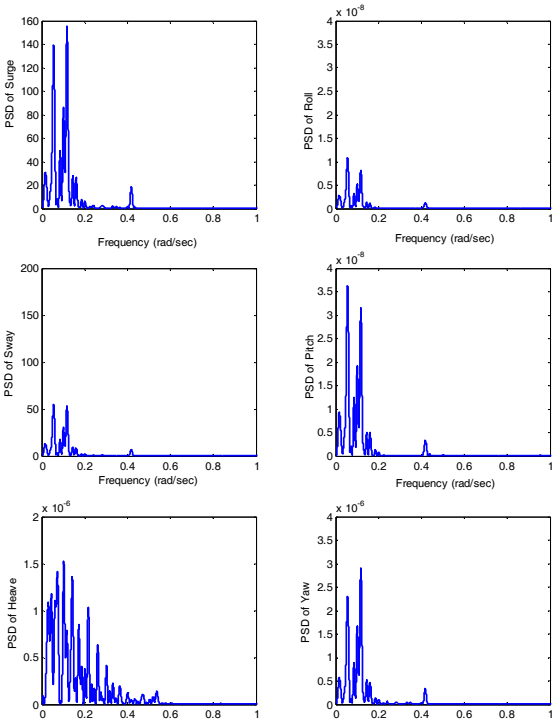

Fig. 10- PSD of displacements

Conclusion

The nonlinear dynamic response of TLP under random sea wave loads was investigated considering nonlinearities. The simple modified Euler method was proposed as a numerical procedure which can be effectively used for the analysis of the dynamic response of structures in time domain for TLPs. The analyses were carried out in both time and frequency domains via a computer program developed for the analysis and design optimization of TLP. The time history of random wave is generated based on Pierson - Moskowitz spectrum and it acts on the structure in arbitrary direction. The hydrodynamic forces are calculated using the modified Morison equation according to Airy's linear wave theory. This kind of analysis is necessary to check the response of designed TLP under environmental loads and fatigue studies as well. Also such results are used to optimization of both hull geometry and tendon pretensions.

References

1-Angelides, D. C., Chen, C., Will, S. A., 1982. Dynamic response of tension leg platform. Proceedings of BOSS 2, 100-120.

2-Morgan, J.R., Malaeb, D., 1983. Dynamic analysis of tension leg platforms. In: Proceedings of the Second International Conference of Offshore Mechanics and Arctic Engineering, Houston, 31-37.

3-Chandrasekaran, S., Jain, A.K., 2001. Nonlinear dynamic behavior of Offshore Tension Leg Platforms under regular wave loads. Ocean Engineering 28 (12).

4-Chandrasekaran, S., Jain, A.K., 2002. Triangular configuration tension leg platform behavior under random sea wave loads. Journal of Ocean Engineering 29, 1985-1928.

5-Hahn, G. D., 1990. A Modified Euler method for dynamic analysis, International Journal for Numerical Methods in Engineering, 32, 943-955.

6-Sanghvi, J. R., 1990. Simplified dynamic analysis of offshore structures, M.S. Thesis, Department of Civil and Environmental Engineering, Vanderbilt University.

7-Tabeshpour, M. R., Golafshani, A. A., and Seif, M. S., (2006), "A Comprehensive study on the results of tension leg platform responses in random sea", Journal of Zhejiang University, Vol. 7, No. 8, pp. 1305-1317.

8-Seif, M. S., Tabeshpour, M. R., and M. Davoodi, A.A. Golafshani (2005), "Geometrical Optimum Design of TLP Using Genetic Algorithm Method", the 1st International Conference on Design Engineering and Science, Vienna, AUSTRIA.

9-Tabeshpour, M.R., Golafshani, A.A., and Seif, M.S., (2006), " Simple Model for Exact Heave Motion of Tension Leg

Platform" WSEAS Transactions on Applied Mathematics, Vol 5., pp. 500-506.

10-Tabeshpour, M.R., Seif, M.S. and Golafshani, A.A., (2004), "Vertical response of TLP with the effect of added mass fluctuation," 16th Symposium on Theory and Practice of Shipbuilding, SORTA 2004, Croatia.

11-Tabeshpour, M.R., Golafshani, A.A., and Seif, M.S., (2005), "The effect of added mass fluctuation on vertical vibration of a TLP", International Journal of Engineering, Vol 18, No 3.

12-Lee, C.P., Lee, J.F., (1993): Wave Induced Surge Motion of a Tension Leg Structure, Ocean Engineering vol. 20, No 2, 171–186.

13-Lee, C.P., (1994): Dragged Surge Motion of a Tension Leg Structure, International Journal of Ocean Engineering vol. 21 No 3, 311-328.

14-Lee, H.H. Wang, P.-W. Lee, C.-P., (1999): Dragged Surge Motion of Tension Leg Platforms and Strained Elastic Tethers, Ocean Engineering vol. 26 No 2, 579–594.

15-Tabeshpour, M.R., Golafshani, A.A., Ataie Ashtiani, B., and Seif, M.S., (2006), "Analytical Solution of Heave Vibration of Tension Leg Platform" Int. J. Hydrology and Hydromechanics Vol. 54, No. 3.

16-M. R. Tabeshpour , B. Ataie Ashtiani , M. S. Seif and A. A. Golafshani, (2006) "Wave Interaction Pitch Response of Tension Leg Structures", 13th International Congress on Sound and Vibration, Austria, Vienna.

17-Tabeshpour, M. R., Golafshani, A. A., and Seif, M. S., (2006), " Convergence and stability of modified Euler method for strongly nonlinear dynamic systems", 14th International Conference on Mechanical Engineering, Isfahan, Iran.